

in Figure 1 and the supplementary material. The cyanohydrin alkoxide complex $(\eta^5\text{-C}_5\text{H}_5)\text{Re}(\text{NO})(\text{PPh}_3)(\text{OCH}(\text{CN})\text{C}_6\text{F}_5)$ (**2a**) formed in quantitative NMR yields as 96–97:3–4 mixtures of (*RS,SR*)/(*RR,SS*) diastereomers.⁸ The dominant diastereomer is consistent with (among possibilities analyzed earlier)^{4,6} CN⁻ attack upon (1) **1a_π** from a direction opposite to rhenium or (2) the trans σ isomer (*E*)-**1a_σ** from a direction opposite to the bulky PPh₃ ligand (Scheme I).

Figure 1 shows that the rate of reaction of **1a_π** depends upon [CN⁻] at lower [CN⁻] but approaches zero order in [CN⁻] at higher [CN⁻]. Such behavior ("saturation kinetics") requires an intermediate⁹ and is readily interpreted in the context of the model in Scheme I and the attendant expression for k_{obs} . First, any residual slope in Figure 1 at high [CN⁻] provides an upper bound on k_{r} , the rate constant for the direct reaction of **1a_π** and CN⁻ to give **2a** ($<7.3 \times 10^{-5} \text{ M}^{-1} \text{ s}^{-1}$). Thus, k_{obs} reduces to $k_1 k_{\sigma} [\text{CN}^-] / (k_{-1} + k_{\sigma} [\text{CN}^-])$, which depending upon the relative magnitudes of k_{-1} and $k_{\sigma} [\text{CN}^-]$ gives either a first- or zero-order dependence upon [CN⁻] (low [CN⁻], k_{σ} rate determining; high [CN⁻], k_1 rate determining). Data can be extracted by a double reciprocal plot of $1/k_{\text{obs}}$ vs $1/[\text{CN}^-]$ (Figure 1 inset), which gives $k_1 = 7.2 \times 10^{-4} \text{ s}^{-1}$ (from the intercept) and $k_{-1}/k_1 k_{\sigma} = 6.9 \text{ Ms}$ (from the slope).¹⁰ If k_1/k_{-1} , the equilibrium constant for **1a_π** \rightleftharpoons **1a_σ** is then assumed to be $<10^{-2}$, then k_{σ} must be $>15 \text{ M}^{-1} \text{ s}^{-1}$. Thus, the relative reactivity of **1a_σ** and **1a_π** toward CN⁻ (k_{σ}/k_{π}) is $>10^5$ in *CDCl₃* at -83°C .

Additional rate experiments were conducted. First, k_{obs} ($\approx k_1$) was measured at [CN⁻] $\geq 0.20 \text{ M}$ at $-78, -83, -88, -93,$ and -98°C . An Eyring plot gave $\Delta H^{\ddagger}_{\text{r}\rightarrow\sigma} = 12.3 \pm 0.3 \text{ kcal/mol}$, and $\Delta S^{\ddagger}_{\text{r}\rightarrow\sigma} = 7 \pm 3 \text{ eu}$. Also, rates of reaction of the *p*-(trifluoromethyl)benzaldehyde complex $[(\eta^5\text{-C}_5\text{H}_5)\text{Re}(\text{NO})(\text{PPh}_3)(\text{O}=\text{CH}-p\text{-C}_6\text{H}_4\text{CF}_3)]^+\text{BF}_4^-$ (**1b**) and PPN^+CN^- showed a similar saturation effect. Complex **1b** exists as a 91:9 mixture of diastereomers (**1b_π**, **1b_σ**), and a small amount of a σ isomer can be detected by UV/visible spectroscopy ($<4\%$ by IR) in CH_2Cl_2 at 26°C .⁵ Accordingly, the rate of disappearance of **1b_π** at high [CN⁻] at -98°C ($k_{\text{obs}} = 1.56 \times 10^{-3} \text{ s}^{-1} \approx k_1$) was 50 times that of **1a_π**.

Rates of reaction of analogous *p*-chlorobenzaldehyde, benzaldehyde, *p*-methylbenzaldehyde, and *p*-methoxybenzaldehyde complexes (**1c,d,e,f**)⁵ with PPN^+CN^- were too fast to measure at -120°C . Thus, competition experiments were conducted with 1:10:10 molar ratios of PPN^+CN^- and pairs of aldehyde complexes. A **1b/1c** mixture gave a 20:80 ratio of the corresponding cyanohydrin alkoxide complexes **2b/2c** (CD_2Cl_2 , in situ, -80°C). Similarly, **1c/1d** and **1d/1e** yielded 35:65 mixtures of **2c/2d** and **2d/2e**. Finally, **1e/1f** gave a $<1:99$ mixture of **2e/2f** (CHCl_2F , -130°C). Thus, the progressively more electron-releasing aryl substituents in this series of compounds enhance the rate of CN⁻ attack, in contrast to the deactivation that might have been intuitively expected. Importantly, however, the equilibrium proportions of σ isomers also increase (π/σ , CH_2Cl_2 , 26°C : **1c,d,e,f** 83:17, 84:16, 53:47, 15:85).^{5a} Hence, this reactivity trend provides further support for the greater electrophilicity of σ isomers.

In summary, the preceding data constitute compelling evidence that σ isomers of **1** are more reactive toward CN⁻ than π isomers. We predict that this result will prove general for a variety of other nucleophiles and Lewis acids. However, Corcoran has recently examined TiCl_4 -catalyzed Diels–Alder reactions of enones containing alkoxy groups capable of promoting π and σ chelates.³ In contrast, he finds enones disposed toward π chelate formation to be more reactive. Finally, the σ adduct manifold in Scheme

I can now be confidently assigned as the progenitor of diastereoselection. However, certain observations suggest other subtleties that must be incorporated into any comprehensive model of the reaction coordinate. Study of these secondary effects is in progress.

Acknowledgment. We thank the NIH for support of this research.

Supplementary Material Available: Experimental procedures and tables of rate and characterization data (3 pages). Ordering information is given on any current masthead page.

Accessibility to the Active Site of Methane Monooxygenase: The First Demonstration of Exogenous Ligand Binding to the Diiron Cluster

Kristoffer K. Andersson,[†] Timothy E. Elgren,[†] Lawrence Que, Jr.,*[‡] and John D. Lipscomb*[‡]

Department of Biochemistry, Medical School and
Department of Chemistry, University of Minnesota
Minneapolis, Minnesota 55455

Received June 19, 1992

Methane monooxygenase (MMO) catalyzes the oxidation of many hydrocarbons.^{1,2} The soluble, 245 kDa methane monooxygenase hydroxylase (MMOH) component from *Methylosinus trichosporium* OB3B contains two diiron clusters believed to be the sites of dioxygen activation.^{1,3} Although the structure of the diiron cluster⁴ in MMOH is not known, spectroscopic^{1,5,6} studies suggest that it is related to, but distinct from, the (μ -oxo)diiron clusters found in hemerythrin^{4,7} and the R2-protein of ribonucleotide reductase.^{4,8} Unlike MMOH, which is colorless,^{1,6c}

* Address correspondence to Prof. J. D. Lipscomb, Department of Biochemistry, 4-225 Millard Hall, University of Minnesota, Minneapolis, MN 55455. Tel (612)-625-6454. Fax (612)-625-2163.

[†] Department of Biochemistry.

[‡] Department of Chemistry.

(1) Fox, B. G.; Froland, W. A.; Dege, J.; Lipscomb, J. D. *J. Biol. Chem.* **1989**, *264*, 10023–10033.

(2) (a) Colby, J.; Stirling, D. I.; Dalton, H. *Biochem. J.* **1977**, *165*, 395–402. (b) Dalton, H. *Adv. Appl. Microbiol.* **1980**, *26*, 71–87. (c) Anthony, C. *The Biochemistry of the Methyloprotophytes*; Academic Press: London, 1982. (d) Green, J.; Dalton, H. *J. Biol. Chem.* **1989**, *264*, 17698–17703. (e) Rataj, M. J.; Kauth, J. E.; Donnelly, M. I. *J. Biol. Chem.* **1991**, *266*, 18684–18690. (f) Froland, W. A.; Andersson, K. K.; Lee, S.-K.; Liu, Y.; Lipscomb, J. D. *J. Biol. Chem.* **1992**, *267*, 17588–17597.

(3) Andersson, K. K.; Froland, W. A.; Lee, S.-K.; Lipscomb, J. D. *New J. Chem.* **1991**, *15*, 411–415.

(4) (a) Sanders-Loehr, J. In *Iron Carriers and Iron Proteins*; Loehr, T. M., Ed.; VCH Publishers: New York, 1989; pp 373–466. (b) Kurtz, D. M. *Chem. Rev.* **1990**, *90*, 585–606. (c) Que, L., Jr.; True, A. E. In *Progress in Inorganic Chemistry*; Lippard, S. J., Ed.; Wiley & Sons: New York, 1990; Vol. 38, pp 97–200. (d) Vincent, J. B.; Olivier-Lilly, G.; Averil, B. A. *Chem. Rev.* **1990**, *90*, 1447–1467.

(5) (a) Woodland, M. P.; Patil, D. S.; Cammack, R.; Dalton, H. *Biochim. Biophys. Acta* **1986**, *873*, 237–242. (b) Fox, B. G.; Surerus, K. K.; Münck, E.; Lipscomb, J. D. *J. Biol. Chem.* **1988**, *263*, 10553–10556. (c) Hendrich, M. P.; Münck, E.; Fox, B. G.; Lipscomb, J. D. *J. Am. Chem. Soc.* **1990**, *112*, 5861–5865.

(6) (a) Prince, R. C.; George, G. N.; Savas, J. C.; Cramer, S. P.; Patel, R. N. *Biochim. Biophys. Acta* **1988**, *952*, 220–229. (b) Ericson, A.; Hedman, B.; Hodgson, K. O.; Green, J.; Dalton, H.; Bentsen, J. G.; Beer, R. H.; Lippard, S. J. *J. Am. Chem. Soc.* **1988**, *110*, 2330–2332. (c) DeWitt, J. G.; Bentsen, J. G.; Rosenzweig, A. C.; Hedman, B.; Green, J.; Pilkington, S.; Papaefthymiou, G. C.; Dalton, H.; Hodgson, K. O.; Lippard, S. J. *J. Am. Chem. Soc.* **1991**, *113*, 9219–9235.

(7) (a) Sheriff, S.; Hendrickson, W. A.; Smith, J. L. *J. Mol. Biol.* **1987**, *197*, 273–296. (b) Holmes, M. A.; Stenkamp, R. E. *J. Mol. Biol.* **1991**, *220*, 723–737. (c) Reem, R. C.; McCormick, J. M.; Richardson, D. E.; Devlin, F. J.; Stephens, P. J.; Musselman, R. L.; Solomon, E. I. *J. Am. Chem. Soc.* **1989**, *111*, 4688–4704.

(8) Nordlund, P.; Sjöberg, B.-M.; Eklund, H. *Nature* **1990**, *345*, 593–598. (b) Petersson, L.; Gräslund, A.; Ehrenberg, A.; Sjöberg, B.-M.; Reichard, P. *J. Biol. Chem.* **1980**, *255*, 6706–6712. (c) Scarrow, R. C.; Maroney, M. J.; Palmer, S. M.; Que, L., Jr.; Roe, A. L.; Salowe, S. P.; Stubbe, J. *J. Am. Chem. Soc.* **1987**, *109*, 7857–7864. (d) Bunker, G.; Petersson, L.; Sjöberg, B.-M.; Sahlin, M.; Chance, M.; Chance, B.; Ehrenberg, A. *Biochemistry* **1987**, *26*, 4708–4716.

(8) Complexes **2a,b** were characterized by NMR (¹H, ¹³C, ³¹P) and IR spectroscopy (supplementary material). Configurational assignments were made by analogy to nine related cyanohydrin alkoxide complexes reported recently.⁶

(9) Huisgen, R. *Angew. Chem., Int. Ed. Engl.* **1970**, *9*, 751.

(10) Note that k_1 denotes the rate of isomerization of **1a_π** to both C=O geometric isomers of **1a_σ** (*E/Z*) and that k_{σ} is the aggregate rate of formation of both diastereomers of **2a** from both isomers of **1a_σ**. Barriers to *E/Z* isomerization in related σ ketone complexes are extremely low ($\Delta G^{\ddagger} = 6\text{--}8 \text{ kcal/mol}$).^{4b} Also, (*RS,SR*)/(*RR,SS*)-**2** ratios include material derived from **1_r**.

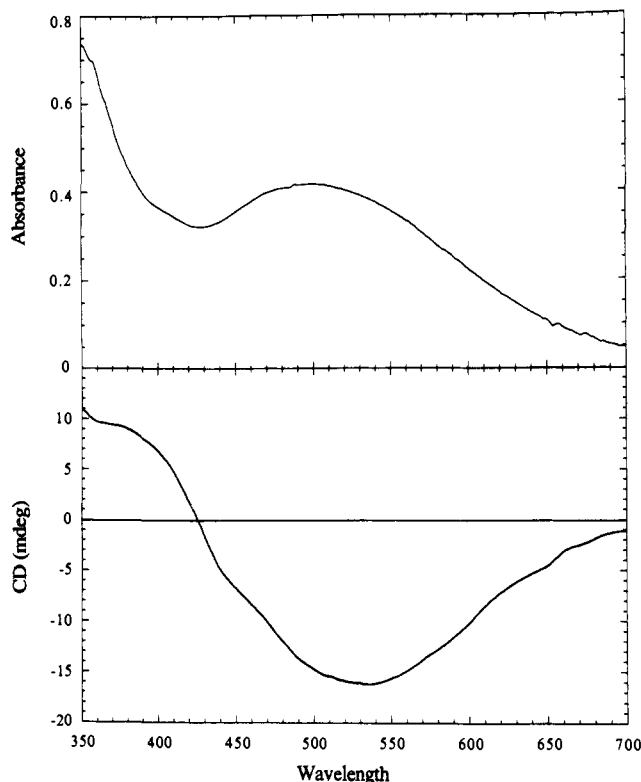


Figure 1. Optical and CD spectra of MMOH-phenol complex. (A, top) Difference optical spectrum at 4 °C and 0.1 M MOPS pH 7.2 of 25 mM phenol + 71 mg of MMOH/mL minus 71 mg of MMOH/mL (MMOH contributed at most 5% of absorbance). Samples were incubated for at least 15 min prior to recording the spectra. (B, bottom) Difference CD spectrum of 25 mM phenol + 71 mg of MMOH/mL minus 71 mg of MMOH/mL. Temperature = 25 °C.

these proteins exhibit weak visible chromophores^{4,7c,8b} due to oxo-Fe charge transfer. A fourth member of this class, purple acid phosphatases,⁹ such as uteroferrin (Uf),^{9b,c,10} exhibits an intense pink or purple color due to charge transfer to Fe(III) from an endogenous tyrosine ligand.¹¹ MMOH represents the only instance where the diiron cluster participates in oxygenase chemistry;^{1,3} consequently, it is of interest to determine its unique structural features. The MMOH active site appears to be open to substrates of different sizes and dimensions;¹⁻³ however, there is no evidence to date of exogenous ligand binding to the diiron cluster. We report here the first direct spectroscopic evidence of such ligation.

Phenol is the sole product of benzene oxidation catalyzed by MMO.^{2a} Addition of phenol ($K_{d,app} \sim 5$ mM) to resting diferric MMOH¹² elicits an optical chromophore at 500 nm ($\epsilon = 0.7$ mM⁻¹ cm⁻¹ per cluster) as shown in Figure 1A. The chromophore observed is similar to, but less intense¹³ than, those observed for

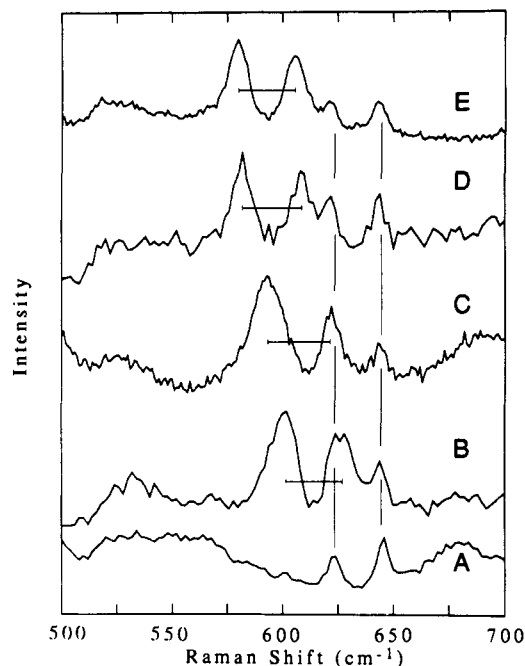


Figure 2. Resonance Raman spectra of MMOH-phenol complexes. Resonance Raman spectra ($\lambda_{ex} = 514.5$ nm) of 150–200 mg MMOH/mL at 4 °C pH 7.2 in the absence and presence of 15–25 mM phenol. Trace (A) resting MMOH, (B) + phenol, (C) + [¹⁸O]-phenol, (D) + [¹³C₆]-phenol, and (E) + [¹⁸O]-phenol-*d*₅.

phenolate-to-Fe(III) charge-transfer (LMCT) transitions of iron-tyrosinate proteins¹⁴ (1.2–4 mM⁻¹ cm⁻¹ per phenolate). However model phenol complexes exhibit extinction coefficients as low as 1 mM⁻¹ cm⁻¹/phenolate ([Fe(HDA)(H₂O)])¹⁵ to as high as 3 mM⁻¹ cm⁻¹/phenolate ([Fe₂O(HDP)₂(benzoate)]⁺).¹⁶ The red color disappears and at least 80% of the original activity is observed after separation of the phenol from MMOH by gel filtration, establishing the reversibility of phenol binding.¹⁷ Low-temperature EPR spectra of the MMOH-phenol complex exhibit no new features, showing that the active site iron remains EPR silent, due to retention of the antiferromagnetic^{5b,c} coupling of the cluster irons. The CD spectrum of the MMOH phenol complex (Figure 1B) contains a negative feature at 530 nm not present in the CD spectrum of MMOH. The presence of an optically active chromophore correlated with phenol binding demonstrates that the red chromophore is formed in the chiral environment of the enzyme.¹⁸

(13) Mössbauer spectra of the enzyme-phenolate complex formed at the phenol concentration used here show that all of the iron clusters are affected by phenol binding and no mononuclear iron sites are formed. Thus, the low extinction coefficient does not result from lack of binding saturation. (Andersson, K. K.; Lipscomb, J. D.; Fox, B. G.; Münck, E. Unpublished observation.)

(14) Que, L., Jr. *Coord. Chem. Rev.* **1983**, *50*, 73–108.

(15) HDA = *N*-(2-hydroxybenzyl)-*N*-(carboxymethyl)glycine: Murch, B. P.; Bradley, F. C.; Boyle, P. D.; Papaefthymiou, V.; Que, L., Jr. *J. Am. Chem. Soc.* **1987**, *109*, 7993–8003.

(16) HDP = *N*-(2-hydroxybenzyl)-*N,N*-bis(2-pyridylmethyl)amine: Yan, S.; Que, L., Jr.; Taylor, L. F.; Anderson, O. P. *J. Am. Chem. Soc.* **1988**, *110*, 5222–5224.

(17) Steady-state kinetic inhibition studies show that phenol rapidly binds to the enzyme, thereby inhibiting furan (a substrate) turnover. In contrast, the chromophoric enzyme complex with phenol described here forms slowly relative to turnover but, once formed, completely inhibits furan turnover until phenol dissociates. It is likely that the former type of inhibition derives from competition with furan for enzyme binding, while the latter type results from direct binding to an accessible site on the iron cluster. Consequently, we believe that the phenol is formed from benzene in one location in the active site and then can migrate to another location near the iron to form the red complex.

(18) In contrast to the red phenol complex, addition of catechol to MMOH generates an intense blue LMCT transition for which there is no CD intensity in the visible region. Nearly all of this blue chromophore can be separated from the protein by gel filtration and thus arises from removal of the active site iron by the catechol.

(9) (a) Averill, B. A.; Davis, J. C.; Burman, S.; Zirino, T.; Sanders-Loehr, J.; Loehr, T. M.; Sage, J. T.; Debrunner, P. G. *J. Am. Chem. Soc.* **1987**, *109*, 3760–3767. (b) Doi, K.; Antanaitis, B. C.; Aisen, P. *Struct. Bonding* **1988**, *70*, 1–26. (c) Vincent, J. B.; Averill, B. A. *FASEB J.* **1990**, *4*, 3009–3014.

(10) (a) Scarrow, R. C.; Pyrz, J. W.; Que, L., Jr. *J. Am. Chem. Soc.* **1990**, *112*, 657–665. (b) David, S. S.; Que, L., Jr. *J. Am. Chem. Soc.* **1990**, *112*, 6455–6463. (c) True, A. E.; Scarrow, R. C.; Holz, R. C.; Que, L., Jr. Submitted for publication.

(11) Antanaitis, B. C.; Streckas, T.; Aisen, P. *J. Biol. Chem.* **1982**, *257*, 3766–3770.

(12) MMOH was purified as described¹ as modified: Fox, B. G.; Froland, W. A.; Jollie, D. R.; Lipscomb, J. D. *Methods Enzymol.* **1990**, *188*, 191–202. Various samples had specific activity of 800–1200 nmol/mg-min and contained 3.8–4.1 Fe per MMOH. Gel filtration experiments after incubation of MMOH with 23 mM phenol or catechol were performed at 4 °C with a small Sephadex G25 column in 100 mM MOPS at pH 7.2. Phenol-*d*₆ was from Isotope Inc., Miamisburg, OH; [¹³C₆]-phenol was from Cambridge Isotope Laboratories, Woburn, MA; [¹⁸O]-phenol was synthesized (according to Orville, A. M.; Harpel, M. R.; Lipscomb, J. D. *Methods Enzymol.* **1990**, *188*, 107–115) and analyzed with GC-MS and ¹H NMR.

Resonance Raman spectra of the MMOH-phenol complex (Figure 2) show definitively that the chromophore arises from a phenolate-to-Fe(III) charge-transfer transition derived from an *exogenous* phenol. Two enhanced features appear at 602 and 628 cm^{-1} (brackets in Figure 2B) using 514.5-nm laser excitation that are absent in the spectra of MMOH (150 mg/mL) (Figure 2A), a buffer/phenol solution, and MMOH-phenol with $\lambda_{\text{ex}} = 632 \text{ nm}$.¹⁹ As expected, the two Raman bands shift to lower frequency for samples prepared with [¹⁸O]-phenol (Figure 2C, 592 and 620 cm^{-1}), [¹³C₆]-phenol (Figure 2D, 582 and 608 cm^{-1}), and [²H₅]-phenol (Figure 2E, 580 and 606 cm^{-1}). The $\sim 26\text{-cm}^{-1}$ separation of the two bands in the MMOH-phenol complex is conserved in each of these spectra indicating that the two vibrational features are similar in origin. The observed isotope shifts indicate that these modes have both significant phenol ring deformation and Fe-O stretching character as observed for *p*-cresolate-Fe(III) and phenol-Fe(III) complexes.²⁰ However these complexes typically exhibit only one mode in this region. Thus the two bands in the MMOH-phenol complex probably arise from two phenolate ligands in distinct environments. At present it is unclear whether these represent two phenols bound to the same diiron cluster or to two slightly different clusters, although the low intensity of the LMCT band might favor the latter interpretation.

The observation of the first visible chromophore of MMOH allows the application of previously inaccessible optical techniques to assess the cluster iron coordination. In general the energy of phenolate-to-Fe(III) LMCT transition reflects the Lewis acidity of the metal center,^{20a,21} which in turn is determined by its ligand environment. The visible and CD absorption of the MMOH-phenol complex are remarkably similar to those of Uf²² which suggests similar cluster ligand environments for the two proteins. The present model^{9b,c,10} for the Uf active site consists of a (μ -hydroxo)diiron unit probably supported by a carboxylate bridge with a tyrosine and a histidine on one iron and a histidine and a carboxylate on the other iron. Such a coordination environment, less the tyrosine, is consistent with ENDOR²³ and EXAFS⁶ studies of uncomplexed MMOH, but the significant difference in intensity between the LMCT bands of MMOH-phenol and Uf indicates subtle differences in ligand environment. The bearing of these structural differences on unique hydrocarbon oxidation chemistry by MMOH is currently the subject of further spectroscopic and kinetic investigation of the phenolate complexes. The demonstration here that relatively large molecules have access to the diiron cluster may also serve to differentiate MMOH from other proteins that contain related clusters.²⁴

(19) The two features are in the metal ligand vibrational region of the Raman spectrum typical of Fe(III)-phenolate complexes.^{9a,b,14,20} The phenolate ring vibrational modes at higher frequencies (1100-1600 cm^{-1}), which are characteristic of iron-tyrosine proteins,¹⁴ are not observed above the protein background; these features may be weak as a result of the low intensity of the MMOH-phenol LMCT band and/or the use of the unsubstituted phenol instead of a para-substituted phenol. In an iron porphyrin phenol complex,^{20b} only the $\sim 600\text{-cm}^{-1}$ feature is unequivocally observed in the Raman spectrum.

(20) (a) Pyrz, J. W.; Roe, A. L.; Stern, L. J.; Que, L., Jr. *J. Am. Chem. Soc.* **1987**, *107*, 614-620. (b) Uno, T.; Hatano, K.; Nishimura, Y.; Arata, Y. *Inorg. Chem.* **1990**, *29*, 2803-2807.

(21) (a) Cox, D. D.; Benkovic, S. J.; Bloom, L. M.; Bradley, F. C.; Nelson, M. J.; Que, L., Jr.; Wallick, D. E. *J. Am. Chem. Soc.* **1988**, *110*, 2026-2032. (b) Andersson, K. K.; Cox, D. D.; Que, L., Jr.; Flatmark, T.; Haavik, J. *J. Biol. Chem.* **1988**, *263*, 18621-18626.

(22) Antanaitis, B. C.; Aisen, P.; Lilienthal, H. R. *J. Biol. Chem.* **1983**, *258*, 3166-3172.

(23) Hendrich, M. P.; Fox, B. G.; Andersson, K. K.; Debrunner, P. G.; Lipscomb, J. D. *J. Biol. Chem.* **1992**, *267*, 261-269.

(24) Ribonucleotide reductase R2-protein has been shown to contain short regions of amino acid sequence homology to MMOH in the cluster binding region suggesting similar cluster ligation.²³ Although exogenous hydrocarbon hydroxylation has not been reported for R2, an endogenous tyrosine placed near the cluster by site specific mutation is hydroxylated. The resulting catechol derivative then appears to bind to the diiron cluster to yield a blue-green chromophore analogous in some ways to the red chromophore described here for MMOH (see: Örmö, M.; deMaré, F.; Regnström, K.; Aberg, A.; Sahlin, M.; Ling, J.; Loehr, T.; Sanders-Loehr, J.; Sjöberg, B.-M. *J. Biol. Chem.* **1992**, *267*, 8711-8714). Thus MMOH-like catalysis may be limited in the case of R2 by site accessibility.

Acknowledgment. This research was supported by the National Institutes of Health (Grant GM 40466, J.D.L.) and the National Science Foundation (DMB-9104669, L.Q.) and a contract from Amoco Corporation (J.D.L.). We thank Professor Clare K. Woodward for use of their CD spectrometer.

Characterization of the CO Binding Site of Carbon Monoxide Dehydrogenase from *Clostridium thermoaceticum* by Infrared Spectroscopy[†]

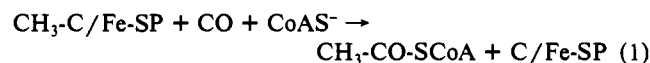
Manoj Kumar and Stephen W. Ragsdale*

Department of Biochemistry, East Campus
University of Nebraska
Lincoln, Nebraska 68583-0718

Received July 9, 1992

This communication describes the results of an infrared spectroscopic study of the binding site for CO on carbon monoxide dehydrogenase (CODH). The CO molecule was found to be terminally coordinated to one metal in the active site mixed metal cluster containing Ni, 3-4 Fe, and acid-labile sulfide. Since CO is not a bridging ligand, there must be an endogenous bridge between Ni and Fe.

The Wood-Ljungdahl pathway is an autotrophic pathway for growth of *Clostridium thermoaceticum* and other anaerobic bacteria in which cell carbon is formed from CO₂, CO, or other organic substrates.¹ CODH catalyzes the final steps in the synthesis of acetyl-CoA from the methylated corrinoid/iron-sulfur protein (CH₃-C/Fe-SP), CO, and coenzyme A (CoA-S⁻) (eq 1). The intermediates are enzyme bound and include methyl-CODH,² carbonyl-CODH,³ and acetyl-CODH^{2,4} (see ref 1a for review). After binding of CoA, thiolytic cleavage of the acetyl group produces acetyl-CoA.⁵



Treatment of CODH with CO reduces the enzyme and elicits an EPR signal with $g_{\perp} = 2.08$ and $g_{\parallel} = 2.028$.⁶ Since this EPR signal is broadened when CODH is enriched with ⁶¹Ni or ⁵⁷Fe and when ¹³CO is reacted with the enzyme,⁷ it has been named the NiFeC signal. The NiFeC species has been shown to be a catalytically competent intermediate in the pathway of acetyl-CoA synthesis.³ EPR,⁷ Mössbauer⁸ and ENDOR^{7c} spectroscopic studies suggest a working model for the structure of the CO binding site as a [NiFe₃-S₄] cluster. Recent work implicates the [NiFe₃-S₄] cluster also serves as the site of methylation and acetylation.^{3,7c}

* For communications regarding this manuscript, please contact: Dr. Stephen W. Ragsdale, Department of Biochemistry, East Campus, University of Nebraska, Lincoln, Nebraska 68583-0718. Phone: 402-472-2943. Facsimile: 402-472-7842.

[†] This manuscript has been assigned Journal Series No. 10019, Agricultural Research Division, University of Nebraska.

(1) (a) Ragsdale, S. W. *CRC Crit. Rev. Biochem. Mol. Biol.* **1991**, *26*, 261-300. (b) Fuchs, G. *FEMS Microbiol. Rev.* **1986**, *39*, 181-213. (c) Ljungdahl, L. G. *Ann. Rev. Microbiol.* **1986**, *40*, 415-450.

(2) Lu, W.-P.; Harder, S. R.; Ragsdale, S. W. *J. Biol. Chem.* **1990**, *265*, 3124-3133.

(3) Gorst, C. M.; Ragsdale, S. W. *J. Biol. Chem.* **1991**, *266*, 20687-20693.

(4) Lu, W.-P.; Ragsdale, S. W. *J. Biol. Chem.* **1991**, *266*, 3554-3564.

(5) (a) Lu, W.-P.; Ragsdale, S. W. *J. Biol. Chem.* **1991**, *266*, 3554-3564.

(b) Ramer, S. E.; Raybuck, S. A.; Orme-Johnson, W. H.; Walsh, C. T. *Biochemistry* **1989**, *28*, 4675-4680.

(6) Ragsdale, S. W.; Ljungdahl, L. G.; DerVartanian, D. V. *Biochem. Biophys. Res. Commun.* **1982**, *108*, 658-663.

(7) (a) Ragsdale, S. W.; Wood, H. G.; Antholine, W. E. *Proc. Natl. Acad. Sci. U.S.A.* **1985**, *82*, 6811-6814. (b) Ragsdale, S. W.; Ljungdahl, L. G.; DerVartanian, D. V. *Biochem. Biophys. Res. Commun.* **1983**, *115*, 658-665.

(c) Fan, C.; Gorst, C. M.; Ragsdale, S. W.; Hoffman, B. M. *Biochemistry* **1991**, *30*, 431-435.

(8) Lindahl, P. A.; Ragsdale, S. W.; Münck, E. J. *Biol. Chem.* **1989**, *265*, 3880-3888.